Research Article

Journal of Labelled Compounds and Radiopharmaceuticals

Received 28 June 2007, Revised 25 August 2007, Accepted 17 September 2007 Published online 2 January 2008 in Wiley Interscience

(www.interscience.wiley.com) DOI: 10.1002/jlcr.1468

Synthesis and preliminary biological evaluation of a ^{99m}Tc-labeled hypericin derivative as a necrosis avid imaging agent

Humphrey Fonge,[a] Lixin Jin,[a] Huaijun Wang,[b] Guy Bormans,[a] Yicheng Ni,[b] and Alfons Verbruggen[a]*

Mono-[^{123}I]iodohypericin and mono-[^{123}I]iodohypericin monocarboxylic acid are iodine-123-labeled hypericin derivatives which have shown great promise in preclinical studies as necrosis avid imaging agents in animal models of infarction. In view of the more attractive properties of a ^{99m}Tc-labeled hypericin derivative, we have synthesized a conjugate of protohypericin monocarboxylic acid with *S*-benzoylmercaptoacetyldiglycyl-diaminopentane in an overall yield of 15%. The conjugate was labeled with technetium-99m by exchange labeling at pH 10 in a labeling yield of 95% followed by photocyclization to yield ^{99m}Tc-mercaptoacetyldiglycyl-1,5-diaminopentylene hypericincarboxamide (^{99m}Tc-13). The negatively charged ^{99m}Tc-13 complex was purified by reversed phase high-pressure liquid chromatography and the log $P_{7.4}$ was determined to be 2.36. In normal NMRI mice, the complex showed slow hepatobiliary clearance while plasma clearance was rapid. The tracer was evaluated in rats with reperfused hepatic infarction by *ex vivo* autoradiography, gamma counting and histochemical techniques. Unlike the radioiodinated hypericin derivatives, the new tracer agent did not show preferential uptake in necrotic tissue on autoradiography and gamma counting techniques. Conjugation of hypericin with a ^{99m}Tc-chelate, resulting in a change in size, charge and lipophilicity, had a profound effect on the necrosis avidity of the tracer agent. The results show that ^{99m}Tc-13 is not suitable for imaging necrosis.

Keywords: necrosis avidity; hypericin; ^{99m}Tc labeling

Introduction

Cell death occurs by two distinct processes, i.e. programmed cell death, called apoptosis and necrosis.[1,2] Necrosis and apoptosis play a central role in the pathogenesis of various disorders and results from different types of insults. Their non-invasive identification and localization are therefore very important in the diagnosis, prognosis and assessment of response to revascularization therapies. This is particularly the case in acute myocardial infarction (AMI) whereby early diagnosis and knowledge of infarct size should permit a timely intervention to salvage the organ as well as to assess response to treatment, which is important for survival and quality of life of the patients.[3,4] ^{99m}Tc-pyrophosphate, ^{111}In/^{99m}Tc-antimyosin Fab antibody and ^{99m}Tc-glucarate have all to some extent been used in nuclear medicine to locate and quantify infarct size[5–7] but none has optimal imaging characteristics. These can be summarized as rapid localization to the infarct, high avidity and specificity for necrotic tissue and reasonable duration of scan positivity.

Our group has been focusing on infarct avid agents for contrast enhancement in magnetic resonance imaging (MRI) and single photon-emission-computed tomography (SPECT).[8–10] We have shown that mono-[^{123}I]iodohypericin ([^{123}I]MIH, Figure 1(A))[9] and mono-[^{123}I]iodohypericin monocarboxylic acid ([^{123}I]MIHA, Figure 1(B))[10] are very avid for necrotic tissue in different animal models of necrosis. However, technetium-99m has more ideal imaging and availability characteristics than iodine-123. Since technetium is a transition metal, labeling requires initial conjugation of hypericin to an appropriate bifunctional chelating agent (BFC). The choice of the BFC is critical in the design of the technetium-labeled tracer agent, because of the alterations in charge, size and lipophilicity introduced by coupling a bioactive compound with some ^{99m}Tc-chelates. This study reports the synthesis of a novel technetium-99m-labeled mercaptoacetyldiglycyl-1,5-diaminopentylene hypericincarboxamide and its evaluation in normal mice and in rats with reperfused hepatic infarction. Tracer uptake in reperfused hepatic infarct was evaluated by *ex vivo* biodistribution studies, autoradiography, triphenyltetrazolium chloride (TTC) and hematoxylin and eosin (H&E) staining techniques for histological correlations.

[a]*Laboratory of Radiopharmacy, Faculty of Pharmaceutical Sciences, K.U. Leuven, BE-3000 Leuven, Belgium*

[b]*Department of Radiology, Faculty of Medicine, K.U. Leuven, BE-3000 Leuven, Belgium*

**Correspondence to: Alfons Verbruggen, Herestraat 49, Onderwijs & Navorsing 2 Box 821, BE-3000 Leuven, Belgium.*
E-mail: alfons.verbruggen@pharm.kuleuven.be

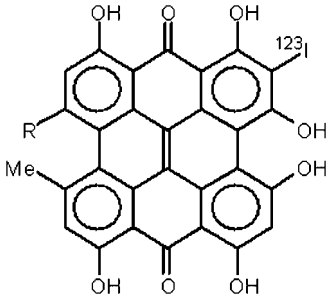

Figure 1. Chemical structures of iodine-123-labeled hypericin derivatives with avidity for necrotic tissue. (A) R = $-CH_3$ = mono-[^{123}I]iodohypericin ([^{123}I]MIH) and (B) R = $-COOH$ = mono[^{123}I]iodohypericin monocarboxylic acid ([^{123}I]MIHA).

Results and discussions

Chemistry and radiolabeling

Scheme 1 shows the synthetic procedure for the selected BFC, *S*-benzoylmercaptoacetyldiglycyl-1,5-diaminopentane. Synthesis of the precursor protohypericin monocarboxylic acid (**9**) was carried out starting from emodin as shown in Scheme 2.[10] Attempts to derivatise hypericin via an acidic phenol (to obtain ether derivatives) at the 'bay region' ($p_{K_a} = 1.7$) resulted in ether conjugates that were unstable under different deprotection conditions and/or during the labeling step. As a result amide derivatives were preferred because of enhanced stability. This was done starting from protohypericin monocarboxylic acid (Scheme 3). Examples of BFCs that were used to derivatize hypericin for labeling with a $[Tc(V)O]^{3+}$ or a $[Tc(CO)_3]^{1+}$ core include: *S*-benzylmercaptoacetyl diaminoethane, *N,N′* bis-BOC triethylene triamine, ethyl iminodiacetate derivatives (ethyl or methyl esters), *S*-benzylmercaptoacetyldiglycyllysine and *S*-benzylmercaptoacetylcysteinyldiglycine. Using *S*-benzylmercaptoacetyl diaminoethane (initially chosen because of enhanced stability of the *S*-benzyl-precursor over the *S*-benzoyl for example) as BFC, the resulting hypericin conjugate, *S*-benzylmercaptoacetyldiglycyl-1,2-diaminoethylene hypericincarboxamide, could not be labeled because of instability under different conditions used to deprotect the thiol group. For this reason, the pentyl linker with an *S*-benzoyl-protected mercaptoacetyldiglycine derivative was chosen as the BFC. The MAG3-like system is known to form a stable complex with technetium-99m. *S*-benzoylmercaptoacetyldiglycine (*S*-Bz-MAG2) was synthesized as reported by Brandau *et al.*,[11] coupled to *N*-BOC substituted 1,5-diaminopentane and after removal of the -BOC protective group the resulting intermediate was conjugated with protohypericin carboxylic acid (Scheme 1, Scheme 2 and Scheme 3). The overall synthetic yield of the novel hypericin derivative (compound **12**) was 15%. This allowed a one-pot deprotection and labeling with a radiochemical yield of 95%. As shown in Figure 2, a reversed phase high-pressure liquid chromatography (RP-HPLC) analysis of the labeling reaction mixture showed the presence of mainly two peaks, probably corresponding to ^{99m}Tc-mercaptoacetyldiglycyl-1,5-diaminopentylene protohypericincarboxamide (^{99m}Tc-proto**13**, $t_R = 32.3$ min) and ^{99m}Tc-mercaptoacetyldiglycyl-1,5-diaminopentylene hypericincarboxamide (^{99m}Tc-**13**, $t_R = 32.5$ min), respectively. Photocyclization necessary to convert ^{99m}Tc-proto**13** to ^{99m}Tc-**13** was done post labeling by irradiating with a 400-W halogen lamp for 30 min. Monitoring of the cyclization reaction using RP-HPLC showed conversion of the mixture of peaks to a

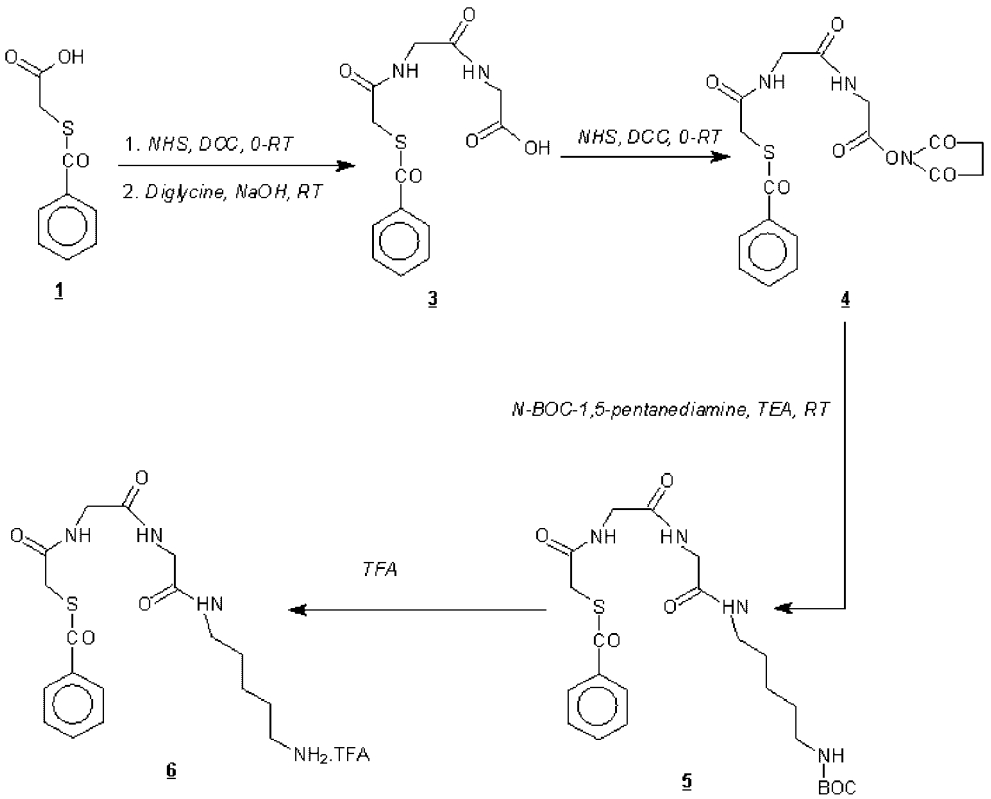

Scheme 1

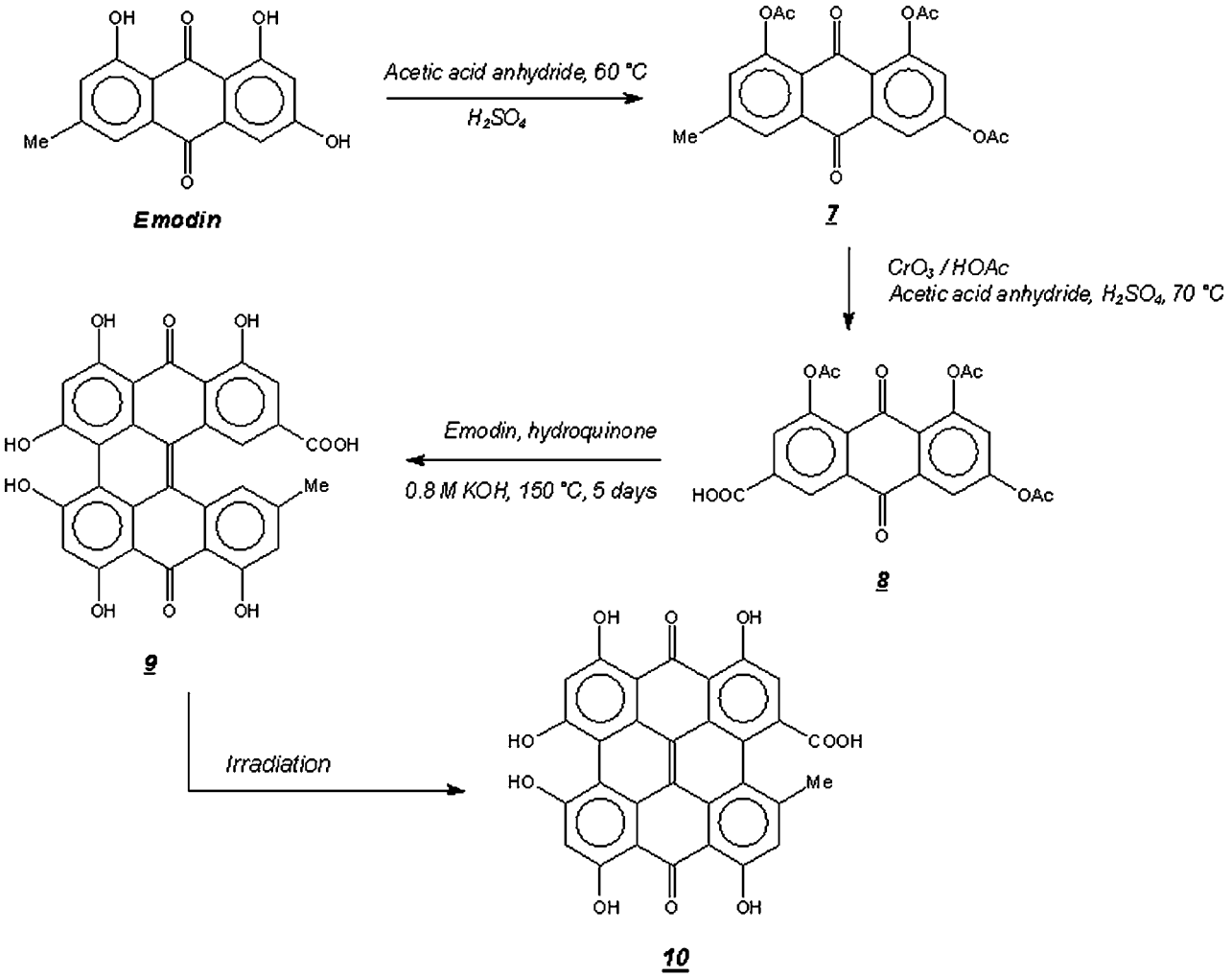

Scheme 2

single peak with a slight shift in retention time for the originally most abundant peak (Figure 2(B)), consistent with the conversion of the radiolabeled protohypericin derivative to the cyclized intended hypericin derivative.

Partition coefficient

The partition coefficient (log $P_{7.4}$) of ^{99m}Tc-**13** was found to be 2.36 ($\pm$0.12). For comparison, the log $P_{7.4}$ of [^{123}I]MIH and [^{123}I]MIHA was previously determined to be 3.08[12] and 1.47[10], respectively.

Biodistribution in normal mice

Biodistribution was evaluated in normal NMRI mice and the results are shown in Table 1. The tracer was slowly cleared via the hepatobiliary pathway resulting in high amounts of tracer in the intestines, amounting to 33 and 63% of injected dose (%ID) at 4 and 24 h post injection (p.i.), respectively. Blood clearance was rapid with only 0.5% ID per gram blood (%ID/g) at 30 min p.i. In previous studies, it was found that [^{123}I]MIH shows high affinity for plasma lipoproteins and has a slow plasma clearance.[13] The faster plasma clearance of ^{99m}Tc-**13** as compared with that of [^{123}I]MIH suggests that ^{99m}Tc-**13** is not significantly bound to plasma lipoproteins. [^{123}I]MIH and [^{123}I]MIHA also showed similar initial high liver uptake, but had a much faster hepatobiliary clearance. Urinary clearance of the new tracer agent was very low.

Necrosis avidity

Necrosis avidity of the tracer was evaluated in rats with reperfused hepatic infarction by *ex vivo* autoradiography and gamma counting in correlation with TTC and H&E staining techniques. The model of reperfused hepatic infarction is preferred in screening experiments of novel compounds to a model of occlusive/reperfused AMI because it is easier to make and because of the fact that very reproducibly an infarct is obtained with a low mortality rate of the animals. Owing to the limited potential clinical applications of the model it therefore serves mainly as a reliable first screening tool.[9,10] Typically, the necrosis/viable liver tissue activity ratio for an avid tracer is low early after injection ($<$4 h p.i.) but increases to a maximum value at later time points ($>$7 h p.i.) due to specific uptake in necrotic tissue and clearance from viable liver tissue.[9] Necrosis was confirmed by TTC staining (TTC negative areas). The images of TTC staining did not fully match with those of autoradiography and H&E staining due to disruptions that occurred during

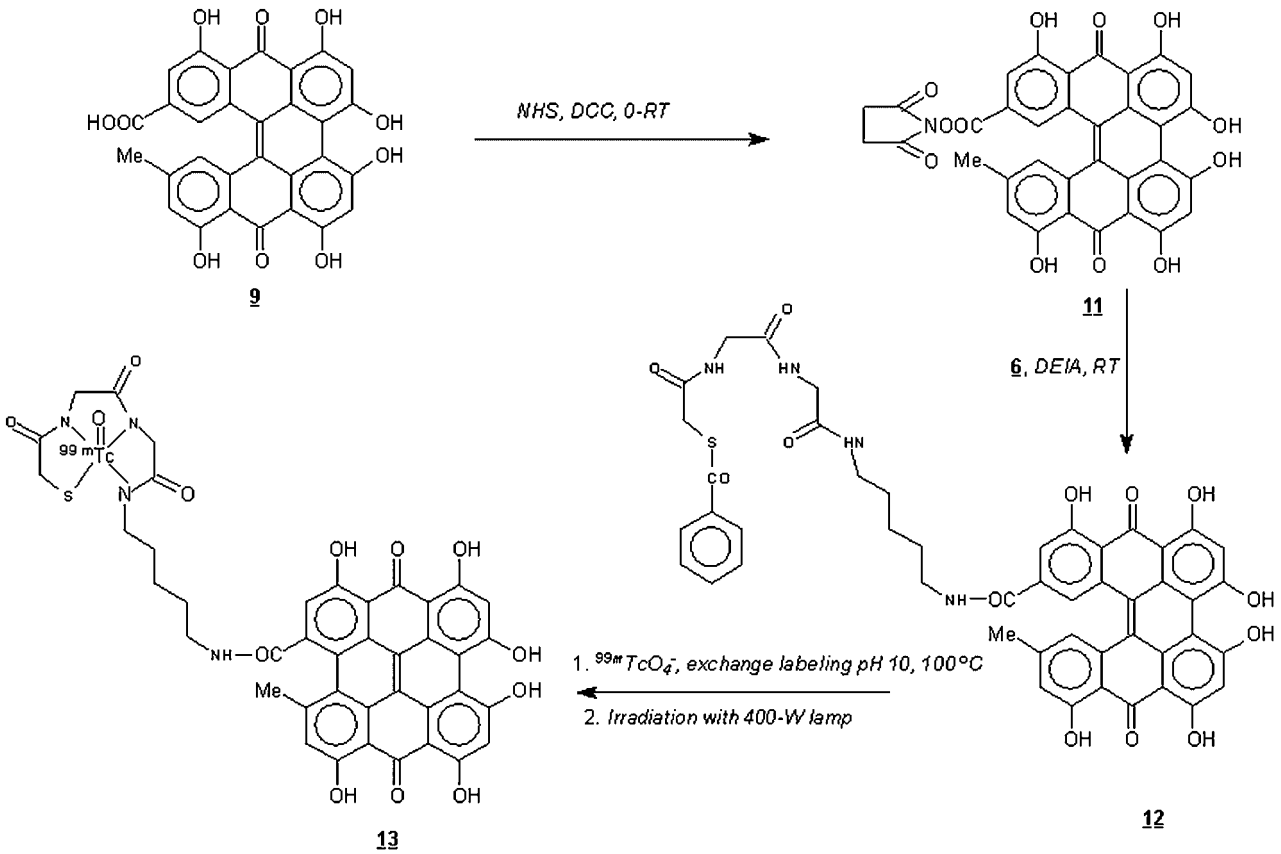

Scheme 3

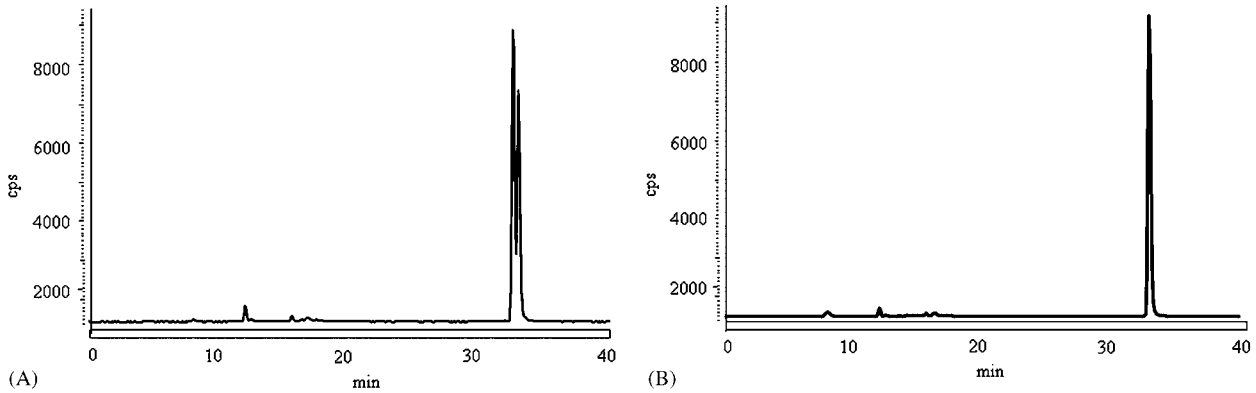

Figure 2. RP-HPLC chromatograms of labeling reaction mixture. (A) ^{99m}Tc-protohypericin derivative (^{99m}Tc-proto**13**, before ring closure) and (B) ^{99m}Tc-hypericin derivative (^{99m}Tc-**13**, after ring closure by irradiation with a 400-W halogen lamp). (See section on instruments for HPLC conditions.)

freezing and microtome sectioning. Region of interest analysis on autoradiograms shows no preferential uptake of tracer in necrotic tissue (Figure 3) at 4 and 24 h p.i. Low uptake in necrotic tissue was also confirmed by gamma counting (necrotic to viable tissue activity ratios were 0.5 and 0.8 at 4 and 24 h p.i., respectively). In rats with reperfused hepatic infarction [^{123}I]MIH showed specific uptake in necrotic tissue with a necrotic to viable tissue activity ratio of 3.1 at 24 h p.i.[14] In reperfused AMI necrotic to viable tissue uptake ratio of [^{123}I]MIH was as high as 81 by autoradiography at 24 h p.i. and myocardial infarction was unequivocally delineated by the tracer at 9 h p.i.[15] [^{123}I]MIHA showed even more favorable characteristics (high avidity and rapid clearance from non-target organs) than [^{123}I]MIH as a necrosis avid imaging agent.[10] The results of the current study indicate that the presence of the ^{99m}Tc-chelate in the new tracer agent has a negative impact on the necrosis avidity, probably as a result of the charge and /or size alterations associated with the conjugation of hypericin with a negatively charged rather bulky chelate. Probably, also a reasonable plasma half-life is a requirement for sufficient accumulation of tracer agents in necrotic tissue.

Table 1. Biodistribution of ^{99m}Tc-mercaptoacetyldiglycyl-1,5-diaminopentylene hypericincarboxamide (^{99m}Tc-**13**) in normal mice ($n \geqslant 3$ per time point)

Organ	% Injected dose (±SD)			% Injected dose/g (±SD)		
	30 min	4 h	24 h	30 min	4 h	24 h
Urine	0.1 (±0.0)	0.7 (±0.9)	2.1 (±1.2)	ND	ND	ND
Kidneys	1.5 (±0.7)	0.8 (±0.0)	0.6 (±0.1)	2.2 (±1.2)	1.8 (±0.0)	1.4 (±0.2)
Liver	75.5 (±3.6)	57.2 (±2.6)	30.6 (±2.6)	36.3 (±3.9)	34.9 (±1.8)	19.4 (±3.1)
Spleen+pancreas	4.4 (±3.0)	3.0 (±0.7)	1.9 (±0.4)	13.4 (±8.4)	14.3 (±4.7)	9.6 (± 3.9)
Lungs	1.7 (±0.2)	0.4 (±0.2)	0.2 (±0.1)	5.3 (±0.6)	2.4 (±0.9)	0.9 (± 0.2)
Heart	1.1 (±0.2)	0.0 (±0.0)	0.0 (±0.0)	0.0 (±0.0)	0.0 (±0.0)	0.0 (±0.0)
Intestines+feces	5.4 (±3.2)	33.3 (±1.1)	62.9 (±2.3)	ND	ND	ND
Stomach	1.9 (±1.4)	1.5 (±1.8)	0.8 (±0.5)	ND	ND	ND
Brain	0.0 (±0.0)	0.0 (±0.0)	0.0 (±0.0)	0.0 (±0.0)	0.0 (±0.0)	0.0 (±0.0)
Blood	0.9 (±0.3)	0.6 (±0.2)	0.1 (±0.1)	0.5 (±0.1)	0.3 (±0.1)	0.1 (±0.1)

Note: ND, not determined; SD, standard deviation.

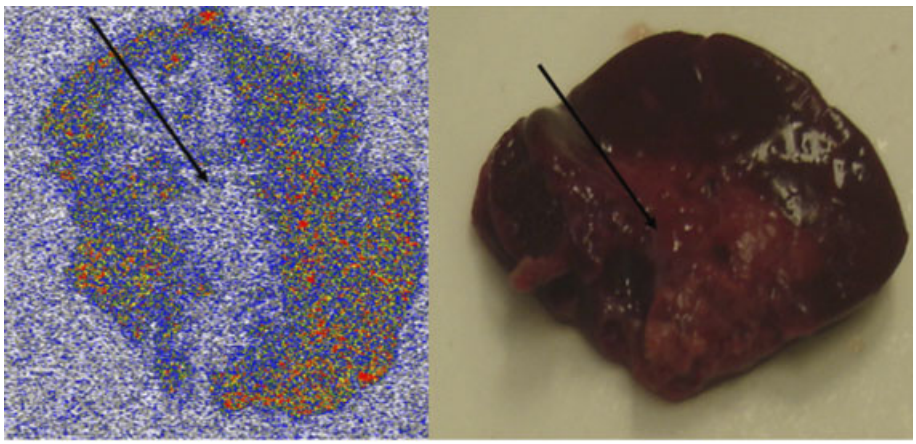

Figure 3. *Ex vivo* analysis of ^{99m}Tc-**13** uptake in rat with reperfused hepatic infarction. (A) Autoradiogram of necrotic liver lobe with low tracer uptake in the necrotic regions (arrow) while adjacent viable tissue shows normal tracer distribution and (B) TTC-stained section of the necrotic liver lobe with arrow pointing to regions of severe necrosis (TTC negative). This figure is available in color online at www.interscience.wiley.com/journal/jlcr.

Experimental procedure

Reagents

Thioglycolic acid, benzoyl chloride, *N*-Boc-1,5-diaminopentane, diglycine, *N*,*N*′-ethyldiisopropylamine, *N*,*N*′-dicyclohexylcarbodiimide and *N*-hydroxysuccinimide were obtained from Sigma Aldrich (Steinheim, Germany). All solvents were obtained from Acros Organics (Geel, Belgium) and were used as purchased. Emodin was a kind gift from Prof. Peter de Witte (Pharmaceutical Biology, K.U. Leuven). Generator eluate containing $Na^{99m}TcO_4$ was obtained from an Ultratechnekow generator (Tyco Healthcare, Petten, The Netherlands).

Instruments

^{1}H NMR spectra were acquired with a Gemini 300 MHz spectrometer (Varian, Palo Alto, CA). Chemical shifts are reported in parts per million (ppm) relative to TMS ($\delta = 0$). Thin-layer chromatography (TLC) was performed on normal phase 0.2-mm thick silica gel 60 plates with UV fluorescence (lot 610/284, Macherey-Nagel, Düren, Germany) and spots were visualized with UV light (Spectroline, Westbury, NY). TLC plates were developed using the following mobile phase systems: system A: toluene/EtOAc/formic acid 50/40/10 V/V or system B: $CHCl_3$/methanol/acetic acid 60/40/1 or system C: CH_2Cl_2/acetone/acetic acid 70/30/1. RP-HPLC analysis was performed on a LaChrom Elite system (Merck-Hitachi, Darmstadt, Germany) using an XTerra RP-C_{18} column (10 μm, 10 mm × 250 mm; Waters, Milford, USA). The compounds were eluted from the column using mixtures of 0.05 M ammonium acetate buffer (pH 6.8) (solvent A) and ethanol (solvent B): 0–10 min: linear gradient from 100% A to 40% A; 10–25 min: 40% A; 25–35 min: linear gradient to 100% B, at a flow rate of 2.2 mL/min over 35 min. The column effluent was monitored using a UV-detector set at 254 nm and the output signal was acquired on a Laura Lite system (Lablogic, Sheffield, UK). For the analysis of radiolabeled compounds, the HPLC eluate was led over a 3-in NaI(Tl) scintillation detector connected to a single-channel analyzer.

Radioactivity counting for biodistribution studies was done using an automated system with a gamma counter (3-in NaI(Tl) well crystal) coupled to a multi-channel analyzer in a sample changer (Wallac, 1480 Wizard® 3′in, Turku, Finland). The results were corrected for background radiation and physical decay during counting. Accurate mass measurement was performed on a time-of-flight mass spectrometer (LCT, Micromass, Manchester, UK) equipped with an electrospray ionization (ESI) interface, operated in positive (ES+) or negative (ES−) mode. Samples were infused in acetonitrile/water using a Harvard 22 syringe pump (Harvard instruments, Massachusetts, USA). Accurate mass determination was performed by co-infusion with a 10 μg/mL solution of a reference as internal calibration standard. Acquisition and processing of data were done using Masslynx software (Micromass, version 3.5).

All animal experiments were conducted with the approval of the institutional ethical committee for conduct of experiments on animals.

Chemistry

N-Hydroxysuccinimidyl-S-benzoylthioglycolate[11] (**2**):
Yield 20.7 g (70.6%). TLC: $R_f = 0.85$ (system C), $R_f = 0.7$ (system B). Accurate mass $[C_{13}H_{10}NO_5S+Na]^+$, theoretical 316.0250 Da, found 316.0258 Da.

S-Benzoylmercaptoacetylglycylglycine[11] (**3**):
Yield 6.75 g (72.2%). TLC: $R_f = 0.1$ (system C). Accurate mass $[C_{13}H_{13}N_2O_5S\text{-}H]^-$, theoretical 309.0551 Da, found 309.0563 Da. ^{1}H NMR (DMSO-d_6) δ 8.5 (t, 1H, CONH), 8.2 (t, 1H, CONH), 7.9–7.5 (m, 5H, ArH), 3.9 (s, 2H, SCH_2) 3.7 (d, 4H, 2 × CH_2).

N-Succinimidyl-S-benzoylmecrcaptoacetylglycylglycine (**4**):
Compound **3** (3.10 g, 0.01 mol) and NHS (1.15 g, 0.01 mol) were dissolved in CH_2Cl_2/DMF 75/25 V/V. The solution was cooled to 0°C and DCC (2.48 g, 0.012 mol) dissolved in 25 mL CH_2Cl_2 was added dropwise while stirring. It was further stirred at 0°C for 1 h and at room temperature (RT) for 16 h. The resulting precipitate was filtered off and washed with CH_2Cl_2/DMF 75/25 V/V. The filtrate was evaporated under reduced pressure and compound **4** was recrystallized from ethyl acetate as a white powder. Yield 3.42 g (84%). TLC: $R_f = 0.4$ (system C). Accurate mass $[C_{17}H_{16}N_3O_7S+Na]^+$ theoretical 430.0679 Da, found 430.0612 Da. ^{1}H NMR (DMSO-d_6) δ 8.6 (t, 2H, 2 × CONH), 7.9–7.5 (m, 5H, ArH), 4.3 (d, 2H, CH_2), 3.9 (s, 2H, SCH_2), 3.8 (d, 2H, CH_2), 2.8 (s, 4H, 2 × $COCH_2$).

S-Benzoylmercaptoacetyldiglycyl-1-amino-5-N-BOC-aminopentane (**5**):
To a solution of compound **4** (1.06 g, 2.6 mmol) in 25 mL THF/DMF 4/1 V/V, a mixture of *N*-Boc-1,5-diaminopentane (0.578 g, 2.86 mmol) and triethylamine (0.41 μL, 3.12 mmol) in 5 mL THF was added with stirring at RT. After stirring overnight, the solvents were evaporated and a white precipitate was obtained after addition of 25 mL water. Yield 1.2 g (93.3%). TLC: $R_f = 0.9$ (system B). Accurate mass $[C_{23}H_{33}N_4O_6S+Na]^+$ theoretical 517.2091 Da, found 517.2123 .Da ^{1}H NMR (DMSO-d_6) δ 8.5–8.2 (m, 4H, 4 × CONH), 7.9–7.4 (m, 5H, ArH), 3.8 (s, 2H, SCH_2), 3.7 (d, 2H, CH_2), 3.6 (d, 2H, CH_2), 3.0–2.8 (m, 4H, 2 × CH_2), 1.7 (d, 4H, 2 × CH_2), 1.4 (s, 9H, 3 × CH_3), 1.2 (m, 2H, CH_2).

S-Benzoylmercaptoacetyldiglycyl-1,5-diaminopentane (**6**):
To a reaction flask under N_2, containing compound **5** (100 mg) at −5°C was added 2 mL TFA. The solution was stirred at −5°C for 20 min and then at RT for 40 min. TFA was evaporated azeotropically with hexane under reduced pressure to give a pale brown oil. Compound **6** was precipitated from the oil after addition of acetonitrile. TLC: $R_f = 0.4$ (system B). Accurate mass $[C_{18}H_{27}N_4O_4S+H]^+$, theoretical 395.1747 Da, found 395.1716 Da.

Tri-acetylemodin[10] (**7**):
The reaction product (compound **7**) consisted of a mixture of di- and tri-acetylated emodin. Yield 99%. Accurate mass di-acetylated emodin $[C_{19}H_{14}O_7\text{-}H]^-$ theoretical 352.0739 Da, found 352.0694 Da.

Tri-acetyl Emodic Acid[10] (**8**):
Yield 98%. Accurate mass of tri-acetylated emodic acid $[C_{21}H_{14}O_{10}\text{-}H]^-$: theoretical 425.0514 Da, found 425.0547 Da.

Protohypericin Monocarboxylic Acid (**9**) *and Hypericin Monocarboxylic Acid* (**10**):
Emodin (0.1 g, 0.37 mmol), compound **8** (0.32 g, 0.75 mmol) and hydroquinone (0.162 g, 1.5 mmol) were dissolved in 5 mL of 0.8 M KOH protected from light in a capped vial placed in a heavy steel reaction vial holder. The vial was placed in an oven at 155°C and allowed to react for 5 days during which it was agitated every 24 h to allow mixing. After cooling, the reaction mixture was acidified to pH 4–4.5 with 1 M HCl and the dark colored precipitate was separated by centrifugation, after which the filtrate was extracted three times with 2% $NaHCO_3$ and EtOAc. The aqueous layer was evaporated *in vacuo* and the residue was dissolved in 25 mL methanol and applied on a silica gel column. Purification was afforded by gradient elution starting from 100% CH_2Cl_2 to CH_2Cl_2/MeOH (80/20 V/V). The first major fraction was collected, evaporated *in vacuo* and repurified on silica gel. Evaporation of solvents yielded the deep purple solid **9**. The residue was dissolved in dry methanol and the solution was irradiated with a 400-W halogen lamp for 30 min to give compound **10**. TLC: $R_f = 0.7$ (system A, compounds **9** and **10**). Accurate mass of **9** $[C_{30}H_{14}O_{10}\text{-}H]^-$ theoretical 533.0510 Da, found 533.0478 Da, accurate mass of **10** $[C_{30}H_{16}O_{10}\text{-}H]^-$ theoretical 535.0703 Da, found 535.0671 Da. ^{1}H NMR **9** (DMSO) δ 7.96 (s, CH-11), 7.67 (s, CH-9), 7.28 (s, CH-14), 7.18 (s, CH-2, CH-5) 6.76 (s, CH-12), 2.50 (s, CH_3).

N-Succinimidyl protohypericin monocarboxylic acid (**11**):
Compound **9** (0.1 g, 0.187 mmol) and NHS (25 mg, 0.22 mmol) were dissolved in THF (20 mL). The solution was cooled to 0°C and DCC (45 mg, 0.22 mmol) dissolved in THF (10 mL) was added dropwise over a 5 min period with stirring. The mixture was further stirred at 0°C for 1 h and then at RT overnight. Dicyclohexyl urea was filtered off and the filtrate evaporated to yield a dark purple residue **11**. Yield 70%. TLC: $R_f = 0.6$ (system A). Accurate mass $[C_{34}H_{18}NO_{12}\text{-}H]^-$ theoretical 682.0834 Da, found 682.0843 Da.

S-Benzoylmercaptoacetyldiglycyl-1,5-diaminopentylene protohypericin-carboxamide (**12**):
To a solution of compound **6** (0.158 g, 0.4 mmol) in 5 mL DMF a solution of compound **11** (0.12 g, 0.187 mmol) and diisopropylethylamine (70 μL, 0.41 mmol) in THF (20 mL) was added dropwise. The reaction mixture was further stirred at RT and monitored on TLC (system A). The reaction was complete after 15 h. The solvents were evaporated under reduced pressure and compound **11** was obtained after two-fold purification on RP-HPLC using an isocratic mobile phase consisting of 0.05 M NH_4OAc/acetonitrile 40/60 V/V, employing a semi-preparative column (XTerra® prep RP_{18} 10 μm, 10 mm × 250 mm) with a flow rate of 2.5 mL/min. Yield 60%. TLC: $R_f = 0.1$ (system A). Accurate mass $[C_{48}H_{38}N_4O_{13}S\text{-}H]^-$, theoretical 911.2240 Da, found 911.2162 Da.

Radiolabeling with technetium-99m

^{99m}Tc-mercaptoacetyldiglycyl-1,5-diaminopentylene hypericincarboxamide (^{99m}Tc-**13**):
Deprotection (removal of the *S*-benzoyl group) and labeling with ^{99m}Tc were achieved in a one-pot reaction by a classical exchange labeling method at pH 10. This was done by consecutively adding 20 mg NaK tartrate in 0.3 mL H_2O, 100 μg stannous chloride dihydrate in 25 μL 0.05 N HCl and 400–600 MBq $Na^{99m}TcO_4$ in 0.3–0.5 mL saline to a solution of 0.5 mg of *S*-benzoylmercaptoacetyldiglycyl-1,5-diaminopentylene protohypericin-carboxamide in 0.3 mL EtOH, buffered with 0.2 mL of 0.5 M phosphate buffer at pH 10. The reaction mixture was heated at 100°C for 20 min followed by irradiation with a 400-W halogen lamp for 30 min in order to cyclize the compound. The labeled compound was purified by RP-HPLC after which the solvents were evaporated by a gently N_2 flush at 40°C prior to formulation in water/polyethylene glycol 400 (PEG 400) 80/20 V/V for biodistribution studies. Reanalysis of the HPLC purified tracer was done by RP-HPLC at different time points post labeling to verify its stability.

Octanol/phosphate buffer partition coefficient

As a measure of the lipophilicity of the RP-HPLC-purified ^{99m}Tc-labeled hypericin derivative, its octanol/phosphate buffer partition coefficient was determined using a modification of the method of Yamauchi *et al.*[16] In a test vial, 50 μL of the HPLC purified radiolabeled compound was mixed with 2 mL of 1-octanol and 2 mL of 0.025 M phosphate buffer pH 7.4. The test vial was vortexed at RT for 2 min and then centrifuged at 1700*g* for 10 min. Approximately 50 μL of the 1-octanol phase and 0.5 mL of the phosphate buffer phase were pipetted into separate tared test tubes with adequate care to avoid cross contamination between the phases. The volume of fluid pipetted was calculated by dividing the net weight of the fluid by its density. The radioactivity of the test tubes was counted using a 3-in NaI(Tl) scintillation detector mounted in a sample changer (Wallac). Corrections were made for background radiation and physical decay during counting. The octanol/buffer partition coefficient, *P*, was calculated using the following equation:

$$P = \frac{\text{cpm/mL in octanol}}{\text{cpm/mL in buffer}}$$

where cpm = counts per min.

Biodistribution in normal mice

Twelve normal NMRI mice ($n = 4$ per time point) weighing 20–32 g were anesthetized by intraperitoneal injection of 0.1 mL of a mixture containing 2.25 mg/mL xylazine hydrochloride and 30 mg/mL ketamine hydrochloride. The mice were injected via a tail vein with 400 kBq of the ^{99m}Tc-hypericin derivative in 0.1 mL water/PEG 400 80/20 V/V and sacrificed by decapitation under anesthesia 30 min, 4 or 24 h p.i. The organs were dissected and weighed in tared tubes and radioactivity in all organs and blood was counted in a gamma counter (Wallac). Corrections were made for background radiation and physical decay during counting. Activity in the organs was expressed as %ID/organ and %ID/g of organ. Activity in blood was calculated on the assumption that blood constitutes 7% of the total body weight.

Evaluation in animal model of hepatic infarction

Rat model of reperfused hepatic infarction: Four adult Wistar rats weighing 350–450 g were anesthetized with i.p. injection of pentobarbital (Nembutal®; Sanofi Santé Animale, Brussels, Belgium) at a dose of 40 mg/kg. Under laparotomy, reperfused hepatic infarction was induced by clamping the hilum of the right liver lobe for 3 h. After reperfusion by declamping hepatic inflow, the abdominal cavity was closed with two-layered sutures and the animals were allowed to recover for at least 8 h. An activity of 18.5–74 MBq of the ^{99m}Tc-labeled hypericin derivative formulated in 0.5 mL water/PEG 400 80/20 V/V was injected via a tail vein and the rats were sacrificed under anesthesia at 4 h ($n = 2$) or 24 h ($n = 2$) p.i. followed by *ex vivo* studies.

Ex vivo studies: For *ex vivo* studies, the necrotic tissues (liver and muscle) and viable control tissues were thoroughly washed with saline (4°C) to remove blood activity. The tissues were then stained separately in TTC solution (1% solution in normal saline) at 37°C for 15 min. Guided by TTC, the necrotic and viable tissues were identified and immediately weighed and activity concentration in the tissues was counted in a 3-in NaI(Tl) scintillation well detector mounted in a sample changer and tracer concentration was expressed as % ID/g tissue or counts per minute (CPM)/g tissue. Digital photographs were taken prior to and after staining. The tissues were then quickly frozen in isopentane cooled in liquid nitrogen and separately cut immediately with a cryotome (Microm HM 550, Walldorf, Germany) into 5–50 μm thick serial sections which then were mounted on slides. Autoradiograms were obtained from these sections by exposing the slides for 2 days to a high-performance phosphor screen (superresolution screen; Canberra-Packard, Meriden, CT). The images were analyzed with Optiquant software (Canberra-Packard) and the activity concentration in the autoradiograms was expressed in digital light units (DLU)/mm^2. The relative tracer concentration in the necrotic and viable sections of the tissues was estimated by regions of interest (ROIs) analysis of the necrotic and the viable regions of 30 and 50-μm thick sections of the autoradiograms of all slices. After exposure for autoradiography, the samples were stained with H&E using a conventional procedure. The H&E stained slices were used to examine microscopic evidence of myocardial necrosis.

Conclusion

The results show that the conjugation of a ^{99m}Tc-chelate to hypericin alters the necrosis avidity of the resulting derivative, presumably because of the changes in lipophilicity, size and charge of the molecule, factors which on their turn may affect residence time in plasma and protein binding. The novel ^{99m}Tc-mercapto-acetyldiglycyl-1,5-diaminopentylene protohypericin-carboxamide is therefore not suitable for visualization of necrotic cell death *in vivo* by SPECT.

Acknowledgement

This work was supported by a grant awarded by Geconcerteerde Onderzoeksactie (GOA) of the Flemish Government, FWO-Vlaanderen (grant G. 0257.05) and in part by the EC-FP6-project DiMI, LSHB-CT-2005-512146.

References

[1] I. Bohm, H. Schild, *Mol. Imaging Biol.* **2003**, *5*, 2–14.
[2] S. Nagata, P. Golstein, *Science* **1995**, *267*, 1449–1456.
[3] B. A. Khaw, *Semin. Nucl. Med.* **1999**, *29*, 259–270.
[4] A. Flotats, I. Carrio, *Eur. J. Nucl. Med. Mol. Imaging* **2003**, *30*, 615–630.
[5] B. A. Khaw, H. W. Strauss, R. Moore, J. T. Fallon, T. Yasuda, H. K. Gold, E. Haber, *J. Nucl. Med.* **1987**, *28*, 76–82.
[6] B. A. Khaw, T. Yasuda, H. K. Gold, R. C. Leinbach, J. A. Johns, M. Kanke, M. Barlai-Kovach, H. W. Strauss, E. Haber, *J. Nucl. Med.* **1987**, *28*, 1671–1678.
[7] G. Mariani, G. Villa, P. F. Rossettin, P. Spallarossa, G. P. Bezante, C. Brunelli, K. Y. Pak, B. A. Khaw, H. W. Strauss, *J. Nucl. Med.* **1999**, *40*, 1832–1839.
[8] Y. Ni, G. Bormans, F. Chen, A. Verbruggen, G. Marchal, *Invest. Radiol.* **2005**, *40*, 526–535.
[9] Y. Ni, D. Huyghe, K. Verbeke, P. A. de Witte, J. Nuyts, L. Mortelmans, F. Chen, G. Marchal, A. M. Verbruggen, G. M. Bormans. *Eur. J. Nucl. Med. Mol. Imaging* **2006**, *33*, 595–601.
[10] H. Fonge, L. Jin, H. Wang, Y. Ni, G. Bormans, A. Verbruggen, *Bioorg. Med. Chem. Lett.* **2007**, *17*, 4001–4005.
[11] W. Brandau, B. Bubeck, M. Eisenhut, D. M. Taylor. *Int. J. Rad. Appl. Instrum. [A]* **1988**, *39*, 121–129.
[12] G. Bormans, D. Huyghe, A. Christiaen, K. Verbeke, T. de Groot, H. Vanbilloen, P. de Witte, A. Verbruggen, *J. Label. Compd. Radiopharm.* **2004**, *47*, 191–198.
[13] H. Fonge, M. Van de Putte, D. Huyghe, G. Bormans, Y. Ni, P. de Witte, A. Verbruggen, *Contrast Media Mol. Imaging* **2007**, *2*, 113–119.
[14] H. A. Fonge, G. Bormans, Y. Ni, F. Chen, K. Verbeke, G. Marchal, L. Mortelmans, A. Verbruggen, *Eur. J. Nucl. Med. Mol. Imaging* **2004**, *31*, S381.
[15] H. Fonge, K. Vunckx, Y. Ni, J. Nuyts, L. Mortelmans, H. Wang, T. de Groot, P. Vermaelen, G. Bormans, A. Verbruggen, Abstract of papers. *Fifty-fourth Annual Meeting of the Society of Nuclear Medicine*, Washington, DC. The Society of Nuclear Medicine, Reston, VA, **2007**, Abstract 610.
[16] H. Yamauchi, J. Takahashi, S. Seri, H. Kawashima, H. Koike, M. Kato-Azuma. *In vitro* and *in vivo* characterisation of a new series of ^{99m}Tc-complexes with N_2S_2 ligands, in *Technetium and Rhenium in Chemistry and Nuclear Medicine* (Eds.: M. Nicolini, G. Bandoli, U. Mazzi), Cortina International, Padova, Italy, **1989**, pp. 475–502.